DESIGN OF A LOW-NOISE AXIAL FAN FOR HEAT PUMP APPLICATIONS

Martina BOLOGNINI, Savino PONTINO
Giuseppe BRUNI, Stefano TORREGIANI

EMC FIME, Via Jesina, 56, Castelfidardo, Italy

SUMMARY

In this paper the design of an axial fan for a heat pump is presented. This technology is experiencing a big growth in the number of applications as they are characterized by low Co2 emissions. The aim of this paper is to present the design of an axial fan able to reach the demanded performance with high efficiency and low noise emissions. The optimization process that leads to an efficient blade is discussed, in order to show the geometry and the fluid-dynamics performances. Then, the resulted blade will be tested by means of numerical simulations to assess the structural and acoustic performances.

INTRODUCTION

The great attention that general public and governments are paying to reducing CO_2 emission is pushing the heat pumps market forward. Indeed, this technology is likely to become the most valid alternative to traditional gas boilers for domestic heating. The great attractiveness of heat pumps therefore also derives from policies aimed at reducing the consumption of fossil fuels and the fight against pollution. Already in the *2020 climate & energy package* drawn up by EU, and subsequently updated in the *Climate Agenda 2030*, the implementation of heat pumps especially in private houses is strongly stimulated. In fact, the main advantage of this technology is due to the fact that, following the current regulations [1], heat pumps work with renewable sources, as the energy stored in air, water, soil is thus considered.

It therefore becomes easy to explain the growth of the heat pump market. The goal is to promote effective energy saving strategies. In this framework Europe represents the reference market: for the policies promoted, sales and production. Moreover, the trend is on the rise. In 2020 Europe recorded an increase in sales of 7.4 % corresponding to 1.62 million units sold. It is estimated that the 6 % of residential buildings are served by heat pumps [2]. Of these, 80 % are expected to be of the air/air or air/water type, which require fans built at the cutting edge of its technology in order to achieve very high efficiency at the working points.

The design process must respect the requirements of performances and must also pay attention to another important feature: low noise. Generally speaking, noise is an incredibly challenging issue for these products. Axial fans are in direct communication with the external environment and there are no shields capable of isolating the fluid-dynamic noise.

The performance and acoustic driven design of an axial fan will be discussed in three main parts: project parameters, fluid-dynamics optimization and verification of structural resistance and acoustic conformity.

PROJECT TARGET

The market analysis on the heat pump producers has been carried out in order to investigate the project parameters required by the motor and impeller. In particular, the performance targets of the heat pump system set the requirements for the axial fan. On the other hand, the geometric and physical characteristics of the heat pump set the constraints. These have to be followed during the entire design process. The optimization of the geometry has been performed on a single working point, that represent the maximum rotational velocity point. It corresponds to a spin rate of 870 rpm and the fan must deliver a certain air flow and guarantee a minimum value of pressure jump. Below the main requirements:

- Impeller diameter: 450 mm
- Number of blades: 3
- Air flow: 3000 m^3/h
- Pressure head $\geq$ 35 Pa
- Nominal speed: 870 RPM
- Power consumption: 115 W

It is very important to respect the requirement on the air flow, as the heat exchanger needs it to work properly. Moreover, keeping the noise level low is another fundamental target of the project. This parameter has been considered as design parameter during the optimization process as well as the other parameters. This will allow choosing the best blades shape under this point of view.

IMPELLER DESIGN

Starting from the data and constraints that have previously been presented it is possible to proceed with the initial stage of the impeller's design, that is, a trial geometry capable of respecting the imposed project targets. The geometry thus generated is going to represent a preliminary shape of the fan that will be analyzed under the point of view of fluid-dynamic and noise performance. Then, this shape will be taken as a reference and will undergo an optimization process in order to better meet the requirements. The geometry definition has been performed through the ADT TurboDesign software, that makes use of numerical methods to generate a suitable shape [3]. The software describes the blade by means of several parameters, that are responsible for directly coupling the geometric features and the fluid-dynamics needs. These parameters represent a sort of *state variables* of the problem, as they can change in a user defined range during an optimization process that takes into account the parameters, the constraints and the desired targets.

Geometric parameters

A brief description [3] of the main parameters of the blade is presented in this paragraph to make it easier to comprehend the following design process.

The thickness of the blade is defined in two ways. The streamwise thickness is the airfoil, that has to be chosen wisely following fluid-dynamics criteria. The spanwise thickness represents the

distribution of the airfoils, if seen as infinitesimal sections, on the length of the blade. This can be selected following either fluid-dynamics and structural requirements, as it can be seen as a thinning of the blade that brings to a taper effect.

The meridional geometry is the bidimensional projection of the solid blade on the radial-axial plane. Defining these parameters allows the user to describe the positions of hub, tip, leading and trailing edges.

The blade loading is one the main parameters influencing the optimization of the shape of the blade. It also plays an important role in the definition of the pressure fields. This has a double definition too. In fact, one can differentiate between spanwise and streamwise blade loading. The spanwise blade loading is mathematically defined as:

$$rV_t^* = rV_\vartheta \cdot \frac{V_{ref}}{r_{ref}} \tag{1}$$

Where r is the generic radial dimension, V_ϑ is the azimuthal velocity, V_{ref} and r_{ref} are respectively the reference velocity and radius. The user must define its distribution between hub and shroud at both the leading and trailing edges. This parameter finds its importance thanks to the Euler Turbomachinery Equation. This stands that the input power can be derived as:

$$P = \dot{m} \cdot \omega \cdot ((\overline{rV_\vartheta})_{TE} - (\overline{rV_\vartheta})_{LE}) \tag{2}$$

Indeed, the spanwise blade loading is also defined as *work coefficient* and is related to power to torque ratio. The typical trend of rV_t^* is the parabolic one for axial fans, considering low values at the hub of the blade.

On the other hand, the streamwise blade loading is mathematically defined as:

$$SWBL = \frac{\partial(rV_\vartheta)}{\partial m} \tag{3}$$

This parameter allows to manage the pressure distribution and in particular the pressure to velocity ratio distribution on the blade surface.

Finally, the stacking is the initial value of the blade wrap angle evaluated along a quasi-orthogonal direction. It represents by line between the center of the blade section at each spanwise location.

First design

The design of the first blade starts from setting likely values for the previously mentioned parameters that are necessary for the appropriate realization of the geometry and to ensure the convergence of the iterative process. In the figure below the streamwise and the spanwise blade loadings are shown as they are set for this very first blade.

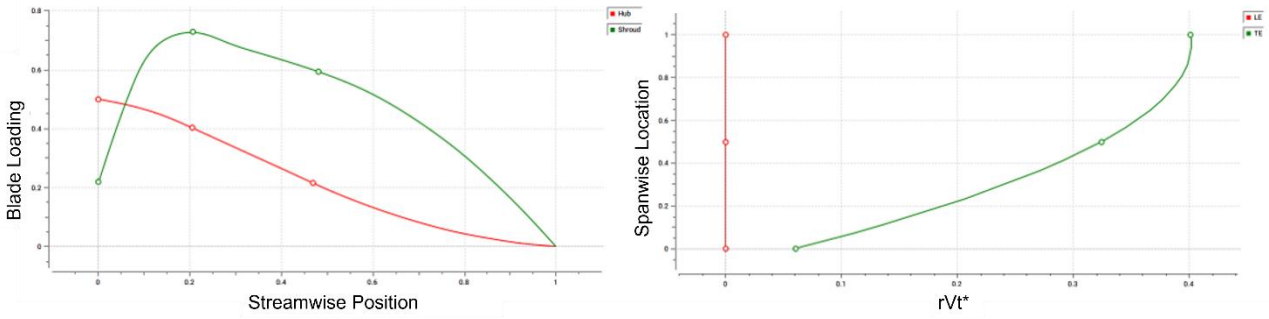

Figure 1: streamwise blade loading (on the left) and spanwise blade loading (on the right)

The image on the left shows the blade loading function of streamwise position for the hub (red line) and for the shroud (green line). The image on the right shows the rV_t^* value along the spanwise location for the LE (red line) and for the TE (green line).

Focusing the attention on the acoustic pressure generated by the impeller in TurboDesign, the first design achieves 52.9 dB of noise. TurboDesign calculates this rotational noise level in a numerical way, by the integration of the Ffowcs Williams and Hawkings equation [4]. The value is the combination of the so-called thickness and loading sound pressure where the thickness noise is related to the blade displacement during the motion and the loading noise is related to the forces that the fluid exerts on the blades. The noise value is examined considering a microphone placed at an axial distance of 1 m from the impeller with a reference frequency of 1000 Hz.

Optimization of the blade

This shape will then be improved thanks to an optimization process that will enhance performance and noise. The optimizer is integrated in the ADT TurboDesign software and is based on Multi Objective Genetic Algorithms capable of evaluating the trade-offs between the parameters. It takes as initial condition the shape of the blade made up by the user setting random parameters. These are then varied by the software in order to obtain the optimized geometries. Ranges of variability have to be defined for the generating point of the TE spanwise, the blade loading at LE ('zero' streamwise location) and the shroud stacking value.

The selected values are listed in Table 1 and show the minimum, the maximum and the base values, corresponding to that of the first blade.

Table 1: range values of the optimization input parameters

Parameter	**Min**	**Base**	**Max**
Spanwise rV_t^* TE hub	0.04	0.06	0.07
Spanwise rV_t^* TE mid	0.30	0.32	0.34
Spanwise rV_t^* TE shroud	0.38	0.40	0.42
Streamwise drV_t^* LE hub	0.2	0.5	0.6
Streamwise drV_t^* LE shroud	0.1	0.22	0.5
Stacking	-5	0	15

The optimization targets are the minimization of torque generated by the impeller, the minimization of the driving force of meridional secondary flow on suction surface and the setting of an acceptable level of total emitted noise. So, 400 designs have been evaluated with several combinations of the parameters. The Pareto Frontier, as output of optimization, is useful in determining the solution that best satisfies the targets. Particular attention is paid to the shroud stacking value. Indeed, if it becomes too negative it generates cavitation phenomena.

In the Table 2 below the main geometric parameters of base and optimized design are presented.

Table 2: comparison of main geometric parameters

Parameter	Unit	Base Design	Optimized Design
LESweep	degrees	-27.1	-29.7
HubLEBAngle	degrees	71.0	66.7
ShrLEBAngle	degrees	72.6	74.0
HubTEBAngle	degrees	35.8	38.6
ShrTEBAngle	degrees	50.2	52.0
HubDiffBAngle	degrees	35.3	28.1
ShrDiffBAngle	degrees	22.4	21.9

In the figure below, the comparison between starting design and the best design is shown.

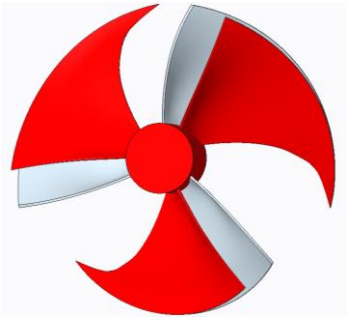

Figure 2: base design (grey) versus optimized geometry (red)

Computational Fluid Dynamics

The fluid-dynamics simulation downstream the process is performed to verify the previously obtained results. The simulation is built in such a way as to consider the axial fan inside the case in the same condition of experimental tests.

Inlet surface are positioned so as to simulate the experimental set-up, the outlet surface is a hemisphere of radius 4 m in order to ensure a good numerical description of the fluid-dynamics far field. The boundaries used for the simulation are stagnation inlet, pressure outlet with constant air density. A RANS model is used both in an initial steady analysis for performance verification and in subsequent URANS simulations for more realistic results and for noise evaluation. The turbulent model used is the $K-\varepsilon$ LagEB, implemented in the software.

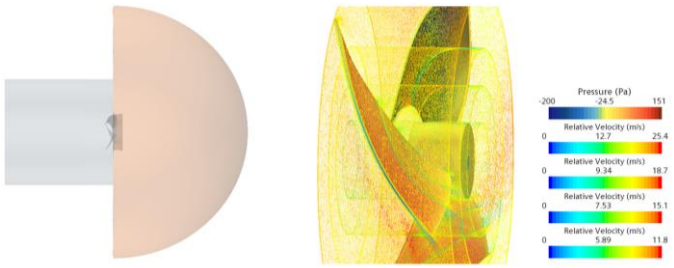

Figure 3: CFD set up and pressure results

Figure 3 shows on the left the fluid domain used for the CFD, on the right the velocity vector plotted on isosurface with different radius and the pressure on the impeller blades.

The results of optimized geometry show that, with the same delivery, the torque decreases by 6.3 %, the driving force of meridional secondary flow decreases by 5.5 % and the noise total emitted noise decrease by 2.6 dB.

STRUCTURAL AND ACOUSTIC ANALYSIS

In the previous chapter the design and the fluid-dynamics performance have been discussed. The CFD results are in accordance with the initial requirements, but the geometry is not yet ready for a test phase. Structural FEM simulations will be presented here to understand if a stiffening of the impeller is necessary or not. Then, through CFD simulations the acoustic spectrum will be evaluated in detail.

Structural analysis

The structural analysis has been carried out with the SIMCENTER 3D software, which exploits the commercial solver NASTRAN. Two types of linear analyses are considered: a static structural one, corresponding to *sol 101*, and a modal analysis according to *sol 103 Real Eigenvalue*.

The solid object was meshed with second order tetrahedral elements of the CTETRA10 type. In order to build a more defined mesh, first a 2D mapped mesh was built on blade surface. The latter was used as a guide for the construction of the 3D final tetrahedral mesh.

The material used for the FEA model is PA 66 GF25 %, with the following structural properties:

- Mass density: $\rho = 1.320$ kg/m³
- Elastic modulus: E = 8400 MPa

At this point it is possible to describe the applied boundary conditions in terms of constrains and loads. The impeller has been constrained as if a shaft were stuck in the hole in the center of rotation.

Two loadings have been applied to the impeller to simulate a realistic working condition. First, a centrifugal load caused by a rotation at 870 rpm has been considered. At the same time the fluid-dynamic load on the blades has been enforced. The static pressure map on the blades has been obtained thanks to the previously described unsteady CFD simulations, as shown in Figure 4.

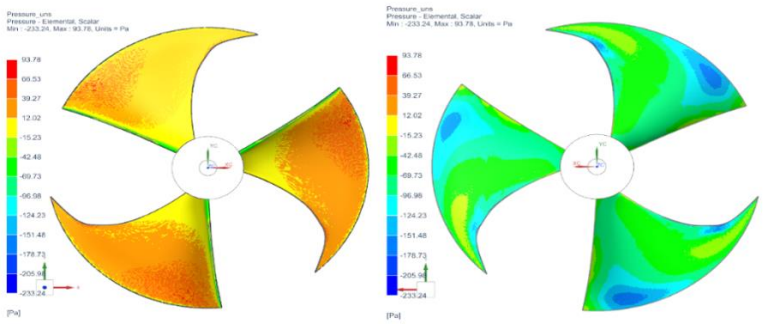

Figure 4: pressure contour on the blade surface. Pressure and suction side

Three structural analyses have been performed: one considering only the centrifugal load, another one with the only static pressure load and a third one where the two loads are applied jointly. In Figure 5 it is possible to see the results of the combined case in terms of displacement and stress according to Von-Mises formulation.

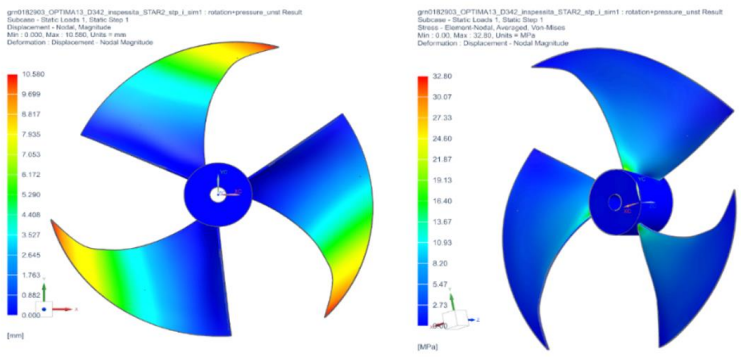

Figure 5: Structural results: displacement and stress contours

Although from the analysis one can notice that the structural effects of the pressure on the blade surfaces is negligible, if compared to that of the centrifugal force, a combined analysis was carried out. The combination of load causes on first thin geometry a displacement of about too large (*16.5 mm*). In order to reduce the displacement a structural optimization study was carried out, with implementation of new geometry, new material and different stiffeners of blade's structure, in according to fluid-dynamics analysis [5]. The final displacement is about 10.6 mm.

A stiffening at the bases of the blades is necessary and a following study focus on the design of the support ribs will be carried on, in order to avoid an excessive deformation.

Modal analysis

The NASTRAN solver *sol 103* has been employed to evaluate the geometry resonance frequencies. In fact, it is well known that, in order to avoid noise and vibration issues when the impeller is in operation, is important to ensure that the structural resonance frequencies do not match with the working frequencies of the system. For a rotating machine there are some noticeable working frequencies that can be predicted in advance. For instance, in this case, the fundamental frequency of the rotation, its third order, due to the number of the blades, or the order corresponding to the magnetic poles of the employed electric motor should be considered.

The modal analysis is performed on the same FEA model described in the previous paragraph, with the same constraints and material. The first six frequencies resulted from the simulation are listed in Table 3.

Table 3: modal analysis results

Mode	Frequency [Hz]
1	41.0
2	41.0
3	41.0
4	101.9
5	102.0
6	102.0

It is important to state that these six modes obviously involve only the blades. In particular, the first three modes have the same frequency and describe the vibration of each one of the three blades. Similarly, the 4, 5, 6 are about the vibration of all the three blades together.

These three results spot out an intersection between the first modes and the working frequency at the maximum speed. Indeed, at 870 rpm the third order frequency is:

$$\frac{870 \text{ rpm}}{60} \times 3 \text{ blades} = 43.5 \text{ Hz}$$

At that velocity the blades are likely to go into resonance, causing noise, vibration, and eventually damage in the structure too. Stiffening the basis of the blades will increase the resonance frequencies of the structure, in accordance with the theory of vibrations.

Acoustic analysis

A transient CFD simulation has been performed to evaluate the noise emissions of the optimized fan geometry. The setup of the numerical analysis doesn't change from the one described in the previous chapter. Some modifications are made regarding the mesh, in order to describe all frequencies of interest. It has been refined near the generation surfaces, which are the blade and the case. The simulation is transient, with the impeller that rotates inside the fluid domain. The rotation has been imposed through a Moving Reference Frame (MRF) with a second order implicit unsteady algorithm with a 9.58×10^{-5} time step. This corresponds to half a degree of rotation per time step. The acoustic pressure fluctuation in the domain is evaluated considering the fluid as incompressible.

First analysis has been carried out with the Ffowcs Williams – Hawkings (FWH) algorithm already integrated in STAR-CCM+ [6]. This simple but effective method splits the noise emitted by a rotating or moving surface in thickness and loading noise. The thickness noise is due to the wave pulse created by the air that is pushed by the movement of the body. The loading noise results from the aerodynamic forces on the surface of the body. The algorithm can also combine these two sources and provide the *total noise*. In Figure 6 it is possible to see the spectra in dB of the three sources.

It is possible to see that the contribution of the loading noise is higher than the thickness one. There is an important peak at 187 Hz that stands out from the graph. This does not correspond to any specific order frequency of the rotating system. However, comparing the value of the peak to the rest of the spectrum, it is possible to say that this could be an outlier caused by a numerical error.

Anyway, the noise level of the rest of the spectrum seems to be comparable to the value provided by TurboDesing.

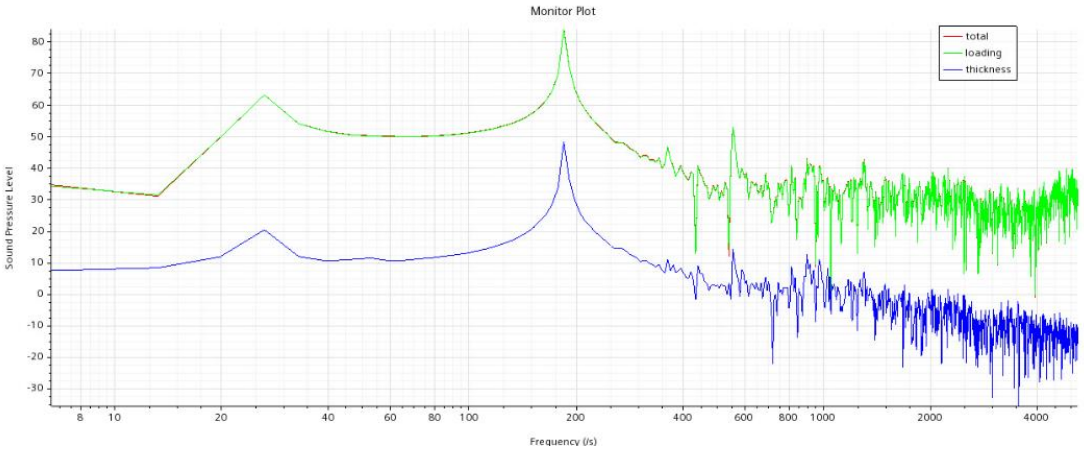

Figure 6: FWH spectrum

More accurate Computational acoustic analysis has been carried out with SIMCENTER 3D software. The simulation uses the CFD data about the distribution of pressure on the fan and case like sources of noise. In order to minimize the computational cost an AML (Automatically Matched

Layer) has been used. In fact, inside the zone limited by AML the acoustic propagation was simulated with FEMAO (FEM Adaptative Order for acoustic elements), that was characterized by expansive numerical operation and by a required 3D mesh. In this case, inside the AML was built a 3D tetrahedral mesh with CETRA 4 first order elements, as shown in figure 7. Outside the AML, the propagation was computed using less expensive numerical methods and mesh was not required.

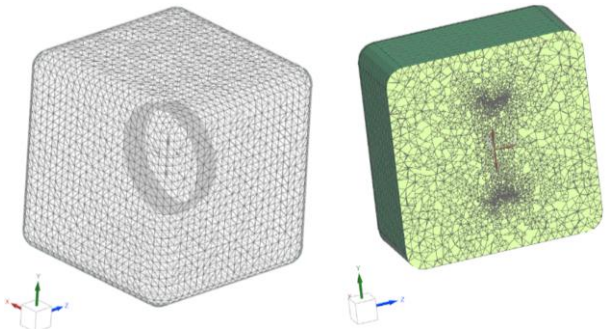

Figure 7: Acoustic Mesh

In order to measure the acoustic pressure was built two microphones plane, across the center plain of domain and one sphere of microphones with radius of 1 meter. The results are shown in figure 8.

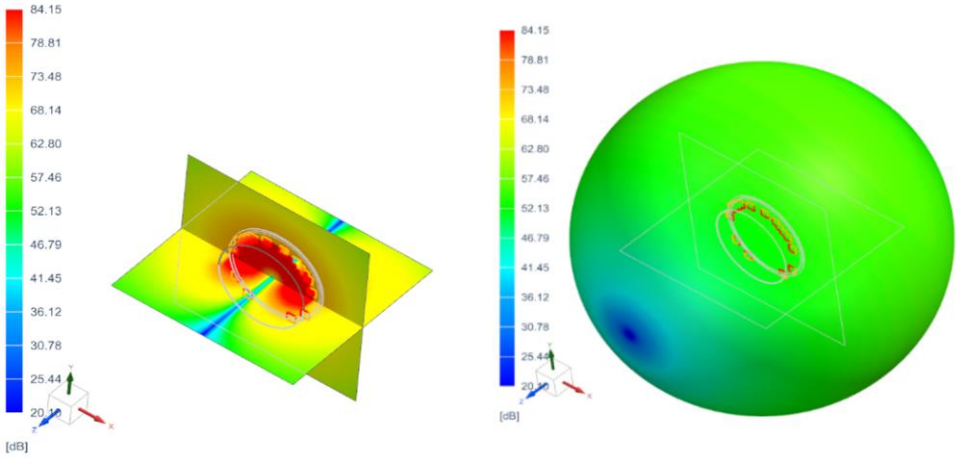

Figure 8: CAA Acoustic Pressure

These results are obtained by sampling the data on 6 revolutions after 6 revolutions employed for initializing the results. At working frequency, 14.5 Hz, if we consider a point at 1 meter of source, on sphere of microphone, there is a sound pressure level of 55 dB, according to the value obtained during the optimization phase.

CONCLUSIONS

The first stages of the design of an axial fan for heat pumps have been described. The performance of the impeller has been evaluated. Under the fluid-dynamics point of view the fan is in line with the requirements and does not need further improvements. On the other hand, the structural analyses hint that the geometry needs structural stiffening in order to avoid deformations and resonances in operation. The results from the acoustic analysis suggest that further improvement must be conducted in order to reduce the noise. Finally, a prototyping of the impeller and laboratory testing will be needed to validate the results and the overall design process.

REFERENCES

[1] Directive (EU) 2018/2001 of the European Parliament and of the Council of 11 December **2018** on the promotion of the use of energy from renewable sources.

[2] European Heat Pump Associations. 2021. *European Heat Pump Market and Statistics Report, **2020***.

[3] ADT. (2021). *TurboDesign User Manual*.

[4] J.E.Ffowcs Williams, D.L. Hawkings, *Sound generation by turbulence and surfaces in arbitrary motion*, Phil. Trans. Roy. Soc. (London) Ser. A, 264, 321 – 342, **1969**

[5] M. Eberlinc, M. Dular, B. Širok, B. Lapanja, *Influence of blade deformation on integral characteristic of axial flow fan*. Journal of Mechanical Engineering. 54, p. 159-169, **2008**.

[6] Siemens Digital Industries Software. Simcenter STAR-CCM+ User Guide, version 2021.2. In *Using the Ffowcs Williams-Hawkings Aeroacoustics Models.* Siemens **2021**.